MECHANICAL CHARACTERIZATION OF FILLER MODIFIED ABS 3D PRINTED COMPOSITES MADE VIA FUSED FILAMENT FABRICATION

A.C. de Mendonça[1], D.K.K. Cavalcanti[1], H.F.M. de Queiroz[1], J.S.S. Neto[1], F.J.P. Chaves[2], M.D Banea[1,3*]

[1]Federal Center of Technological Education in Rio de Janeiro, Brazil
[2]Instituto Politécnico do Cávado e do Ave, Barcelos, Portugal
[3] CICECO - Aveiro Institute of Materials, Department of Materials and Ceramic Engineering, University of Aveiro, 3810-193 Aveiro, Portugal
*Corresponding author's e-mail address: mdbanea@gmail.com

ABSTRACT

Rapid prototyping (also known as additive manufacturing, AM) is a quickly developing process with increasing new applications in a large variety of industrial sectors (i.e., aerospace, automotive, medical, among others.) However, despite the great advantage of a decoupled price to part complexity of an AM fabricated structure, the material properties (largely governed by filament material and printing parameters) still present a significant limiting factor. In this context, the development of new filament materials for a wider range of applications has great potential. In this study, the influence of micro-scale filler reinforcement (powders), both natural (curauá) and synthetic (glass fibre), in the fabrication of an Acrylonitrile Butadiene Styrene (ABS) filament was evaluated. The filler was controlled by weight fraction (~1%) and the filament was fabricated via extrusion. A commercially available 3D printer was used to print tensile and flexural specimens for mechanical characterization as per ASTM standards. The fracture morphology was analysed after tensile testing via optical microscopy in order to evaluate the effect of the fillers on the material deposition and void formation. No significant variation in the tensile properties was reported, except for the strain at failure, while more significant flexural strength variation was observed as a function of filler material. The fillers presented a significant effect on the void density of the fractured surface. It was demonstrated that this simple fabrication technique can generate novel filament materials that may enhance the mechanical properties or widen the range of application (e.g., faster decomposition times in nature for single-use plastics due to the hydrophilic nature of the natural filler and lower water absorption of the hydrophobic synthetic filler for marine environment applications).

KEYWORDS: additive manufactured parts; ABS, fillers, mechanical properties.

1. INTRODUCTION

Rapid prototyping (also known as additive manufacturing, AM) is a fabrication technique in which a part is made via layer-by-layer material deposition or resin photopolymerization. In this way, high-complexity parts can be quickly fabricated at a very low cost [1], [2].

The most widely used technology of this kind is the Fused Filament Fabrication (FFF), sometimes also referred to as Fused Deposition Modelling (FDM) [1], [3], [4]. The main advantage of this process lies in the fact that the design complexity is decoupled from the price. However, the bottleneck is found in the limitation of the material properties of the used filament (thermoplastic) [5], [6]. There are a variety of techniques available that address this problem [2], [5], [7] - [12]. However, high complexity and expensive machinery (i.e., continuous synthetic long-fibre printers) are significant limiting factors. Therefore, there is a need in the current literature to address techniques to possibly improve the filament material properties or widen the range of applications by creating new materials. Furthermore, the printing parameters and the filament polymer play crucial roles in the final mechanical properties of the printed part. These parameters and their influence have been widely studied in the literature [13], [14]. Regarding the improvement of the mechanical properties, one such possibility is the use of fibre reinforcements.

Date of submission/acceptance: 12.09.2022/15.12.2022 https://doi.org/10.35219/awet.2022.02

Natural fibres are among some of the most promising materials that have been used in a wide range of engineering applications. Their aim is not only to improve mechanical properties, but also decrease the weight, cost, and carbon footprint of the structures [2], [15]-[18]. In this context, the application of natural fibre reinforcements with commonly used thermoplastic materials in FDM (i.e., Polylactic Acid (PLA) and Acrylonitrile Butadiene Styrene (ABS)) presents great potential. Another significant factor is the scale of the reinforcements. It is well known that long fibres in the direction of the main loading in a fibre-reinforced structure (composite) are the best-case scenario [8]. However, given the great complexity and need for all-new tooling for such a technique, the possibility of micro-scale reinforcement (powders) infused directly into the filament during the extrusion process is a logical first step.

For example, Safka et al. [19] studied ABS reinforced with coconut and showed that the resulting composite presented a slight increase in tensile modulus (+6%) and a drastic reduction in strength (−50%) and strain (−15%) compared to a neat ABS. Daver et al. [20] studied cork powder modified PLA specimens and found reduced tensile modulus, strength, and impact strength of printed PLA composites. On the other hand, Zander et al. [21] have found an increase in tensile modulus of approximately 60% for Polypropylene PP/10% wood flour and 20% for PP/cardboard compared to neat PP. However, a decrease in tensile strength of 7 to 20% for PP/paper waste fibres and for PP/cardboard fibres was found. Xiao et al. [22] also found a reduction in tensile strength of about 20% by adding hemp hurds in PLA.

In this study, the main objective was the fabrication and characterization of novel micro-scale natural and synthetic fibre-reinforced ABS thermoplastic filaments. The materials were characterized in tensile and flexural tests and a morphological fracture analysis was carried out via optical microscopy.

2. MATERIALS AND METHODS

2.1. Materials

The ABS material used in this work was provided by BASF GP22 ABS in pellet form. Pure curauá powder was used as a second reinforcement phase (in-natura curauá long fibers were supplied by the Federal University of Pará (Pará, Brazil)). The filler was fabricated by first shredding long curauá fibers, then using a ball milling machine (MA 500, MARCONI, SP) for 6h with ball sizes of 12, 10 and 2 mm in diameter. The milled fillers were then filtered using an ASTM 14 mesh 12 sieve. No chemical treatment was used on the fillers. They were stored in a hermetically sealed container since fabrication. No drying was done before filament fabrication. The glass powder used is a commercially available micro-scale reinforcement.

2.2. Filament Fabrication

The filament was produced by a common extrusion process using an extrusion machine Filmaq3D supplied by GTMax3D (Americana, SP, Brazil). The fillers and the ABS material were manually mixed and heated together for 3 minutes at 80ºC. It is known that filament production is an important step in additive manufacturing fabrication. Any defect that occurs at this stage (e.g. porosity) is transferred to the 3D-printed specimens [23], [24]. The weight fraction of the fillers relative to the pellets was approx. 1%. The extrusion process can be seen in figure 1.

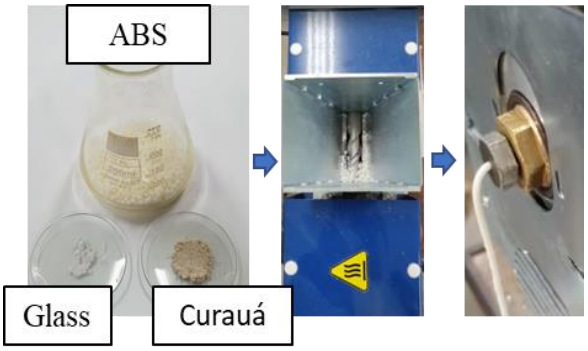

Fig. 1. Filament extrusion process

2.3. Specimen Fabrication

The 3D-printed specimens were fabricated using a Core A1v2 3D printer form GTMax3D (Americana, SP, Brazil). The printing process parameters used in this work are presented in table 1 and were chosen based on the literature and some in-house laboratory trials. The printing process can be seen in figure 2.

Table 1. Printing parameters used [24]

Printing Parameters	Value
Nozzle diameter [mm]	0.40
Layer height [mm]	0.30
Raster width [mm]	0.44
Raster angle	0°
Infill %	100
Extruder temperature [C°]	250
Printing bed temperature [C°]	120
Printing speed [mm/s]	45
Number of contours	44

The printing speed used was 45 mm/s, as it was shown in the literature. This printing speed presented the best results by providing increased diffusion, larger interfacial width and lower internal voids. The slower speed also allows a longer exposure to heat, increasing diffusion between rasters and layers [10]. Finally, the extruder and bed temperature values used were chosen based on the fact that the temperature has a significant impact on the part's properties. A continuous rise in material properties was observed as the nozzle temperature increased, while the bed temperature (i.e. 120 ºC) was chosen to reduce a possible temperature gradient between the top and bottom layers [11].

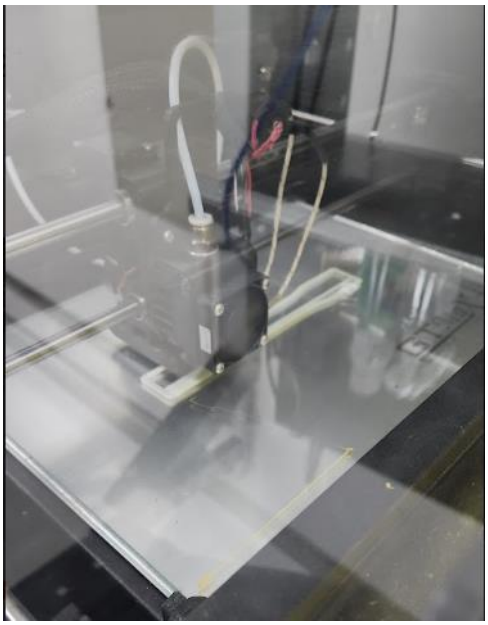

Fig. 2. 3D printing process fabrication of AM specimens

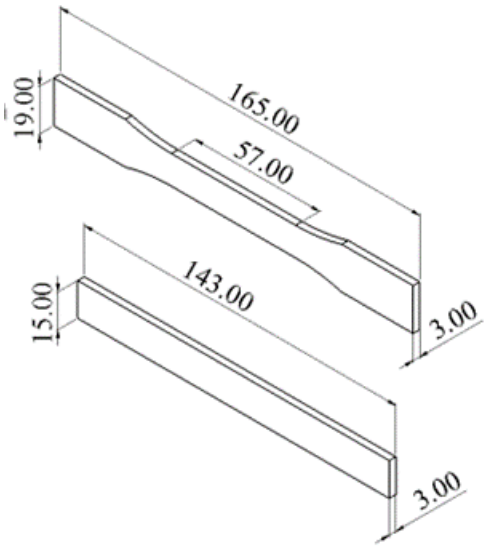

Fig. 3. Scheme of the specimens (dimmensions in milimetres)

Slicing was performed with Simplify3D® and all test specimens were fabricated in a flat-edge orientation. The specimen dimensions (in mm) can be seen in figure 3. Photos of AM fabricated specimens can be seen in figure 4, variations were within 5% in all dimensions.

a)

b)

Fig. 4. Photos of AM parts specimens: a) tensile; b) flexural

Fig. 5. Tensile test set-up

2.4. Test Method

Tensile and flexural tests were performed at room temperature using a testing machine INSTRON® model 5966 (Norwood, Massachusetts, USA). The tensile tests were done with a crosshead speed of 2 mm/min and a load cell of 10kN. A strain gauge extensometer was also used to record the strain. For the flexural tests, a three-point bending rig with a span of 116 mm, crosshead speed of 1 mm/min and a 1 kN load cell were used, as per ASTM D790 standard (specimen span to depth ratio of 1:32). At least three specimens were tested for each condition. The tensile test set up can be seen in figure 5.

Table 2. Tensile properties of the tested specimens

Material	Tensile strength [MPa]	Young's modulus [GPa]	Strain at failure [mm/mm]
Neat-ABS	35.76 ±0.07	1.99 ± 0.004	0.02 ± 0.008
ABS+ Curauá	35.51 ± 0.60	1.99 ± 0.04	0.06 ± 0.017
ABS+ Glass	33.13 ± 0.24	1.96 ± 0.005	0.037 ± 0.02

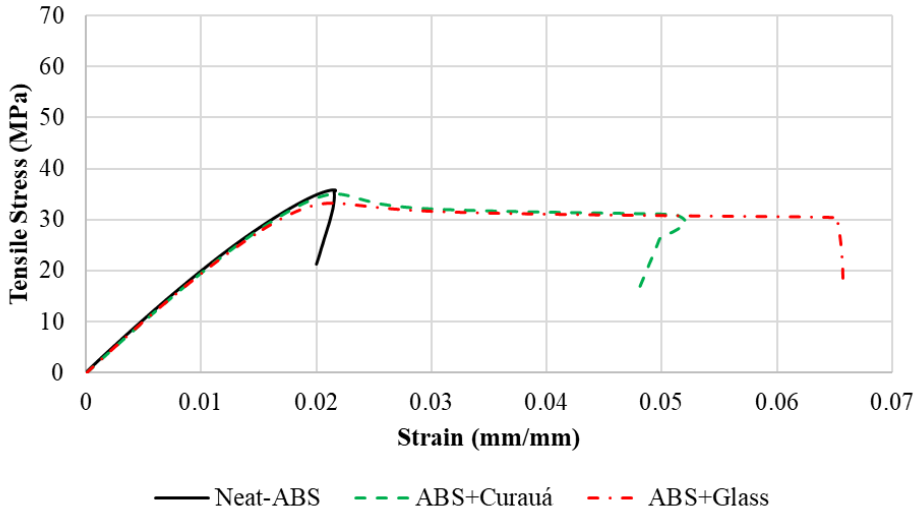

Fig. 6. Representative tensile stress-strain curves as a function of filler material

3. RESULTS AND DISCUSSION

3.1. Tensile tests

Figure 6 shows representative tensile stress-strain curves obtained from the tensile tests of the FDM parts as a function of the material. From the stress/strain curves, the tensile data was calculated (tensile strength, Young's modulus and elongation at break), and the results are presented in table 2.

From figure 6 it can be seen that the behaviour up to the failure of the materials was initially similar. That is echoed in the material stiffness, where little variation was reported. However, the strain at failure varied significantly. This will be further discussed as a function of the failure modes. In Table 2, the quantitative data of the tensile tests can be seen. The tensile strength of all tested materials did not present a significant variation. For example, the Neat-ABS presented a variation in tensile strength of approx. 1% and 7% when compared to the curauá and glass specimens. Regarding Young's modulus, similar variations were reported. This demonstrates that the present technique is capable of fabricating filler-reinforced specimens without deleterious effects of the tensile properties.

In the literature, it is well known that the presence of fillers exhibits a strong tendency to significantly decrease the properties [2], [25].

The strain at reported failure variations was significant. For example, the elongation of the ABS-Curauá and Glass specimens was higher when compared to the Neat-ABS (approx. 67% and 46%). However, the standard deviations were significant due to the specimen failure morphology (Fig. 7).

It can be seen in figure 7, that the tensile failure morphology of the tested specimens varied significantly. From Fig. 7a, the failure cross-section of the Neat-ABS specimens can be seen and the filament deposition pattern (similar to half-circles) can be clearly observed. Furthermore, the voids depicting the deposition spacing can also be clearly

seen (the triangle-shaped voids). Finally, the rough surface of the failure propagation across the deposited filaments displays the characteristic ductile behaviour of the ABS material [23].

In figure 7b, the morphology of the ABS-Curauá tensile failure can be observed. A very different failure mode is found in these specimens. The deposition voids are less uniform and significant voids are observed.

These voids are within the deposited filaments, sometimes almost completely hollowing out the semi-circle. This observation would be consistent with a significant decrease in tensile properties as it is well known that voids within any material under tensile loading will generate local stress concentrators and therefore, crack nucleation sites.

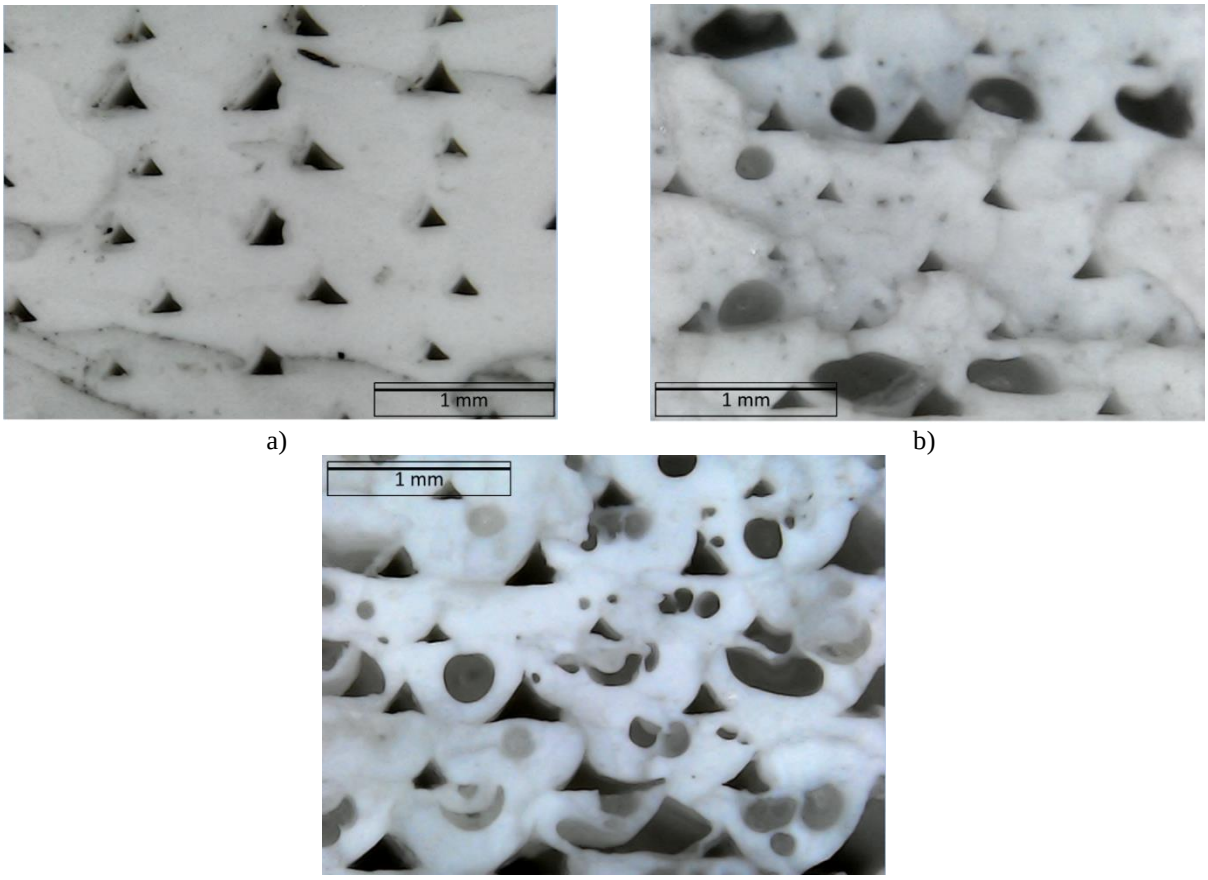

a) b)

c)

Fig. 7. Representative tensile failures of: a) cross-section of Neat-ABS specimen; b) ABS+Curauá specimen; c) ABS+Glass specimen

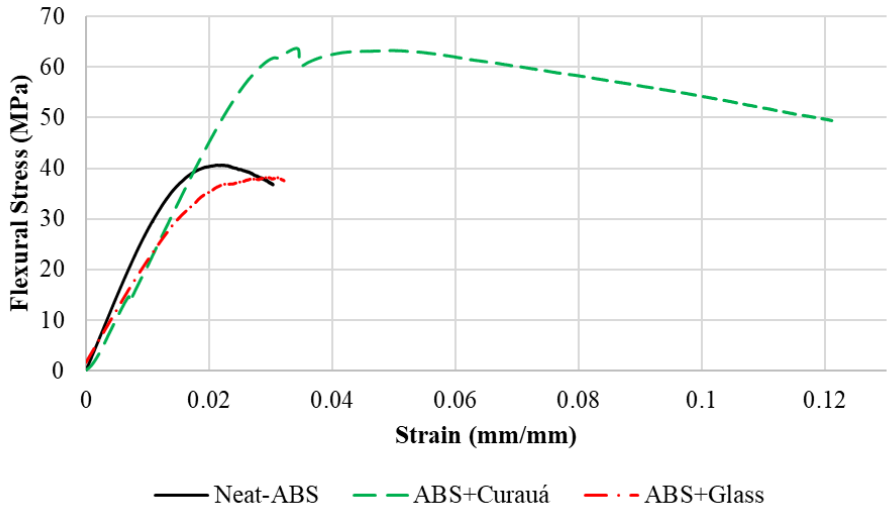

Fig. 8. Representative flexural stress-strain curves as a function of filler material

Table 3. Flexural properties of the tested specimens

Material	Flexural strength [MPa]	Flexural modulus [GPa]
Neat-ABS	37.36 ±4.67	2.23 ± 0.91
ABS+ Curauá	48.31 ± 11.96	1.7 ± 0.13
ABS+Glass	34.17 ± 5.82	1.87 ± 0.30

However, as previously reported, the tensile properties (strength and stiffness) did not significantly decrease, when compared to the Neat-ABS specimens. Therefore, it is concluded that the failure mode variation was more expressly seen in the elongation at failure. There, more random stress states, as a function of the voids, generated failures at different elongation values.

Water is likely the reason for the voids within the ABS-Curauá specimens. The natural fillers did not undergo any chemical treatments nor were they oven-dried prior to filament fabrication (they were stored in hermetically sealed containers since fabrication). However, it is well known that the molecular components of natural fibres (i.e., hemicellulose and cellulose) are highly hydrophilic [10]. Therefore, during specimen printing, the water evaporated, and the gas expansion created localized voids. This indicates that the curauá fillers presented a very good fibre/matrix interface with the ABS since even with a number of voids that may be qualitatively described as nearly catastrophic (e.g., entire depositions hollowed out), the material properties still matched the unfilled case.

Therefore, the application of these fillers with ABS has great potential with careful pre-drying of the fillers in order to remove as much water, as possible as well as chemical treatments to decrease moisture uptake after filament extrusion.

In figure7b, the failure surface morphology of the ABS-Glass specimens can be seen. A similar situation to the curauá specimens is observed, however, an even higher void density can be seen. Differently from the natural fillers, the glass particles are not hydrophilic and the explanation for the voids is likely to be found in the dispersion of the fillers. Given the propensity for the synthetic fillers to form agglomerates if not dispersed homogeneously within the extruded filaments, localized glass particle clumps may form. During specimen printing, these agglomerates will obstruct the correct material flow and consequently, voids will form randomly.

The addition of natural fillers within the current work had little to no impact on the tensile properties of the tested specimens. These results can be considered positive since the current literature states that in general, the addition of natural fillers will tend to reduce the tensile properties of the materials [26]. This indicates that the fillers had a good quality interface with the matrix.

3.2. Flexural Tests

Figure 8 presents representative flexural stress-strain curves of the AM parts as a function of the material. From the stress/strain curves, the flexural data was calculated and presented in table 3.

Similar to the tensile behaviour up to failure, the initial behaviour of the specimens did not vary significantly. However, a more pronounced angle variation (stiffness) is observed. This is confirmed in the quantitative data in table 3. All specimens presented a dominantly ductile behaviour due to the primary phase being ABS.

In table 3, the quantitative flexural properties can be seen. The variation in the flexural properties was more significant than the tensile properties. This is due to the fact that in flexural loading, the top and bottom layers are going to be under maximum compressive and tensile stresses. The variations in flexural strength when the Neat-ABS is compared to the curauá and glass specimens were approx. 33% and 9%. However, it is reported that the standard deviations were significant, especially for the curauá specimens, due to the random distribution of voids and variation in filler/matrix interface quality [2]. Despite this, the curauá specimens presented a significant improvement in flexural strength, echoing the previous observation that the interface quality was overall good and able to counter the effect of the voids in the tensile properties. Similarly, for the glass specimens, the small decrease in the properties is likely to be linked to the higher void density.

Regarding the flexural modulus, the variations when the Neat-ABS is compared to the curauá and glass specimens were approx. 31% and 19%. However, given the high deviation in the Neat-ABS specimens (likely due to printing variations from filament thickness) no definite statistical variation conclusion may be drawn.

The failure mode of all specimens was tensile (crack propagation on the bottom face). This is due to the fact that the ABS presents a higher resistance to compression than traction [27], [28].

Similar to the tensile properties, the flexural properties presented a different trend when compared to the literature, where the flexural strength presented a tendency to decrease, and the flexural modulus presented a tendency to increase [26]. This is due to higher filler interface properties and void content. In flexural properties, the void content will impact the rigidity of the specimens, higher contents being detrimental.

4. CONCLUSIONS

In this work, the mechanical behaviour of filler-reinforced ABS composites made via fused deposition modelling was investigated. Two different fillers (curauá and glass fibre powder) with 1% concentration in filler weight percentage were used to fabricate the Neat and filler-modified ABS filaments. Tensile and flexural tests in accordance with their respective ASTM standards were performed. The following conclusions can be drawn:

- The tensile properties were mostly unaltered by the presence of the fillers. After careful analysis of the fracture morphology of the failed surface, a significant presence of voids was found for both filled cases for different reasons. Significant improvements to the tensile properties may be achieved with careful natural filler drying before the fabrication of the filament and higher filler dispersion homogeneity.
- Significant improvement to flexural strength is possible given the apparent high quality of the curauá/ABS interface. Further improvements are expected with filler drying and chemical treatments, in order to remove hydrophilic contents and low molecular weight waxes.
- The application of natural and synthetic fillers in ABS filaments still presents many challenges but even a simple process can generate significant improvements. This research also gives insight regarding the possibility to use natural fillers for single-use plastics, in order to leverage the hydrophilicity of natural fibres for faster degradation of the plastic in nature, promoting its biodegradation. On the other hand, for the synthetic fillers, much lower water uptake is expected given the hydrophobicity of glass for plastics with application in humid environments without any significant material property loss.

ACKNOWLEDGEMENTS

Authors would like to acknowledge the support of the Brazilian Research Agencies CNPq and FAPERJ.

REFERENCES

[1]. ******* Standard A. F2792. 2012, *Standard terminology for additive manufacturing technologies*, ASTM F2792-10e1, 2012, p. 24.
[2]. **Le Duigou A., Correa D., Ueda M., Matsuzaki R., Castro M.**, *A review of 3D and 4D printing of natural fibre biocomposites*, Materials & Design, 2020, vol. 194, p. 108911.
[3]. **Ngo T.D., Kashani A., Imbalzano G., Nguyen K.T.Q., Hui D.**, *Additive manufacturing (3D printing): A review of materials, methods, applications and challenges*, Composites Part B: Engineering, 2018, vol. 143, pp. 172-196.
[4]. **Popescu D., Zapciu A., Amza C., Baciu F., Marinescu R.,** *FDM process parameters influence over the mechanical properties of polymer specimens: A review*, Polymer Testing, 2018, vol. 69, pp. 157-166.
[5]. **Zhuo P., Li S., Ashcroft I.A., Jones A.I.**, Material extrusion additive manufacturing of continuous fibre reinforced polymer matrix composites: A review and outlook, Composites Part B: Engineering, 2021, vol. 224, p. 109143.
[6]. **Solomon A., Rosenthal Y., Ashkenazi D., Stern A.**, *Structure and mechanical behavior of additive manufactured fused deposition modeling ABS*, Annals of "Dunarea de Jos" University of Galati. Fascicle XII, Welding Equipment and Technology, 2018, vol. 29, pp. 47-56.
[7]. **Ning F., Cong W., Hu Y., Wang H.**, *Additive manufacturing of carbon fiber-reinforced plastic composites using fused deposition modeling: Effects of process parameters on tensile properties*, Journal of Composite Materials, 2017, vol. 51, iss. 4, pp. 451-462.
[8]. **Justo, J., L. Távara, L. García-Guzmán, and F. París**, *Characterization of 3D printed long fibre reinforced composites*, Composite Structures, 2018, vol. 185, pp. 537-548.
[9]. **Taborda-Ríos J.A., López-Botello O., Zambrano-Robledo P., Reyes-Osorio L.A., Garza C.**, *Mechanical characterisation of a bamboo fibre/polylactic acid composite produced by fused deposition modelling*, Journal of Reinforced Plastics and Composites, 2020, vol. 39, iss. 23-24, pp. 932-944.
[10]. **Neto J., Queiroz H., Aguiar R., Lima R., Cavalcanti D., Banea M.D.,** *A review of recent advances in hybrid natural fiber reinforced polymer composites*, Journal of Renewable Materials, 2022, vol. 10, iss. 3, pp. 561-589.
[11]. **Carrasco F., Pagès P., Gámez-Pérez J., Santana O.O., Maspoch M. L.**, *Processing of poly(lactic acid): Characterization of chemical structure, thermal stability and mechanical properties*, Polymer Degradation and Stability, 2010, vol. 95, iss. 2, pp. 116-125.
[12]. **Camargo J. C., Machado Á.R., Almeida E.C., Silva E. F. M. S.**, *Mechanical properties of PLA-graphene filament for FDM 3D printing*, The International Journal of Advanced Manufacturing Technology, 2019, vol. 103, iss. 5, pp. 2423-2443.
[13]. **Peterson A.M.**, *Review of acrylonitrile butadiene styrene in fused filament fabrication: A plastics engineering-focused perspective*, Additive Manufacturing, 2019, vol. 27, pp. 363-371.
[14]. **Ferretti P., Leon-Cardenas C., Santi G. M., Sali M., Ciotti E., Frizziero L., Donnici G., Liverani A.**, *Relationship between FDM 3D Printing Parameters Study: Parameter Optimization for Lower Defects*, Polymers, 2021, vol. 13, iss. 13, p. 2190.
[15]. **Na H., Huang J., Xu H., Bao X., Xie L., Liu F., Zhu B., Wang J., Zhu J.**, *Effect of high content filling jute fiber with large aspect ratio on structure and properties of PLA composite*, Polymer Composites, 2022, vol. 43, iss. 3, pp. 1429-1437.
[16]. **Silva C. G., Campini P. A. L., Rocha D. B., Rosa D. S.**, *The influence of treated eucalyptus microfibers on the properties of PLA biocomposites*, Composites Science and Technology, 2019, vol. 179, pp. 54-62.
[17]. **Zhang K., Chen Z., Smith L. M., Hong G., W. Song, Zhang S.**, *Polypyrrole-modified bamboo fiber/polylactic acid with enhanced mechanical, the antistatic properties and thermal stability*, Industrial Crops and Products, 2021, vol. 162, p. 113227.
[18]. **Yu T., Li Y., Ren J.**, *Preparation and properties of short natural fiber reinforced poly(lactic acid) composites*, Transactions of Nonferrous Metals Society of China, 2009, vol. 19, pp. s651-s655.
[19]. **Šafka J., Ackermann M., Bobek J., Seidl M., Habr J., Běhálek L.**, *Use of Composite Materials for FDM 3D Print Technology*, Materials Science Forum, 2016, vol. 862, pp. 174-181.
[20]. **Daver F., Lee K. P. M., Brandt M., R. Shanks, Cork**, *Cork-PLA composite filaments for fused deposition modelling*, Composites Science and Technology, 2018, vol. 168, pp. 230-237.
[21]. **Zander N.E., Park J. H., Boelter Z. R., Gillan M.A.**, *Recycled Cellulose Polypropylene Composite Feedstocks for Material Extrusion Additive Manufacturing*, ACS Omega, 2019, vol. 4, iss. 9, pp. 13879-13888.
[22]. **Xiao X., Chevali V. S., Song P., D. He, Wang H.**, *Polylactide/hemp hurd biocomposites as sustainable 3D printing feedstock*, Composites Science and Technology, 2019, vol. 184, pp. 107887.
[23]. **Cavalcanti D., Banea M. D., Queiroz H.**, *Mechanical Characterization of Bonded Joints Made of Additive Manufactured Adherends*, Annals of "Dunarea de Jos" University of Galati, Fascicle XII, Welding Equipment and Technology, 2019, vol. 30, pp. 27-33.

[24]. **Cavalcanti D., Banea M.D., Queiroz H. D.**, *Effect of Material on the Mechanical Properties of Additive Manufactured Thermoplastic Parts*, Annals of "Dunarea de Jos" University of Galati. Fascicle XII, Welding Equipment and Technology, 2020, vol. 31, pp. 5-12.
[25]. **Queiroz H. F. M., Banea M. D., Kawasaki K., Cavalcanti D., de Souza e Silva Neto J.,** *The effect of multiscale hybridization on the mechanical properties of natural fiber-reinforced composites*, Journal of Applied Polymer Science, 2021, vol. 138, iss. 41, p. 51213.
[26]. **Mazzanti V., Malagutti L., Mollica F.**, *FDM 3D Printing of Polymers Containing Natural Fillers: A Review of their Mechanical Properties*, Polymers, 2019, vol. 11, iss. 7, p. 1094.
[27]. **Brischetto S., Ferro C. G., Maggiore P., Torre R.**, *Compression Tests of ABS Specimens for UAV Components Produced via the FDM Technique*, Technologies, 2017, vol. 5, iss. 2, p. 20.
[28]. **Oudah S.A., Al-Attraqchi H.B., Nassir N.A.**, *The Effect of Process Parameters on the Compression Property of Acrylonitrile Butadiene Styrene Produced by 3D Printer*, Engineering and Technology Journal, 2022, vol. 40, iss. 1, pp. 189-194.